

# Representing Positional Information in Generative World Models for Object Manipulation

Stefano Ferraro<sup>1</sup>

Pietro Mazzaglia<sup>1</sup>

Tim Verbelen<sup>2</sup>

Bart Dhoedt<sup>1</sup>

Sai Rajeswar<sup>3</sup>

<sup>1</sup> Ghent University, <sup>2</sup> VERSES, <sup>3</sup> ServiceNow  
stefano.ferraro@ugent.be

## Abstract

Object manipulation capabilities are essential skills that set apart embodied agents engaging with the world, especially in the realm of robotics. The ability to predict outcomes of interactions with objects is paramount in this setting. While model-based control methods have started to be employed for tackling manipulation tasks, they have faced challenges in accurately manipulating objects. As we analyze the causes of this limitation, we identify the cause of underperformance in the way current world models represent crucial positional information, especially about the target’s goal specification for object positioning tasks. We introduce a general approach that empowers world model-based agents to effectively solve object-positioning tasks. We propose two declinations of this approach for generative world models: position-conditioned (PCP) and latent-conditioned (LCP) policy learning. In particular, LCP employs object-centric latent representations that explicitly capture object positional information for goal specification. This naturally leads to the emergence of multimodal capabilities, enabling the specification of goals through spatial coordinates or a visual goal. Our methods are rigorously evaluated across several manipulation environments, showing favorable performance compared to current model-based control approaches.

## Introduction

For robotic manipulators, replicating the tasks that humans perform is extremely challenging, due to the complex interactions between the agent and the environment. In recent years, deep reinforcement learning (RL) has emerged as a promising approach for addressing these challenging scenarios (Levine et al. 2016; OpenAI et al. 2019; Kalashnikov et al. 2018; Lu et al. 2021; Lee et al. 2021). Among RL algorithms, model-based approaches aim to provide greater data efficiency compared to their model-free counterparts (Fujimoto, van Hoof, and Meger 2018; Haarnoja et al. 2018). With the advent of world models (WM) (Ha and Schmidhuber 2018), model-based agents have demonstrated impressive performance across various domains (Hafner et al. 2020; Rajeswar et al. 2023; Hafner et al. 2023; Hansen, Wang, and Su 2022; Hansen, Su, and Wang 2024; Lancaster et al. 2024), including real-world robotic applications (Wu et al. 2022; Seo et al. 2023).

Copyright © 2025, Association for the Advancement of Artificial Intelligence (www.aaai.org). All rights reserved.

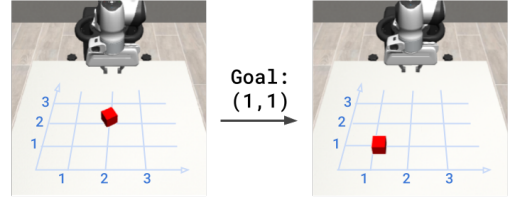


Figure 1: Object positioning task with coordinates goal.

When considering object manipulation tasks, it seems natural to consider an object-centric approach to world modeling. Object-centric world models, like FOCUS (Ferraro et al. 2023) learn a distinct dynamical latent representation **per object**. This contrasts with the popular Dreamer method (Hafner et al. 2023), where a single **flat** representation, referring to the whole scene is extracted.

Model-based generative agents, like Dreamer and FOCUS, learn a latent model of the environment dynamics by reconstructing the agent’s observations and use it to generate latent sequences for learning a behavior policy in imagination (Hafner et al. 2020, 2021, 2023). However, these kinds of agents have shown consistent issues in succeeding in object manipulation tasks, both from proprioceptive/vector inputs (Hansen, Su, and Wang 2024) and from images (Seo et al. 2022). For instance, in the *Shelf Place* task from Metaworld (Yu et al. 2019), DreamerV3’s success rate after 2M steps oscillates around 25% when other approaches, such as the simpler SAC baseline (Haarnoja et al. 2018), quickly reach 100% success, as reported in (Hansen, Su, and Wang 2024).

In this work, we aim to study this failure mode of generative model-based agents and propose a set of solutions that alleviate these issues in existing world models. To be able to perform controlled experiments, in a simple but widely used setup, we focus on the *visual object positioning* problem. As shown in Figure 1, in this setting, at each timestep, the agent receives a visual observation, which shows what the current scene looks like, and a goal target, representing where an object should be moved. Notably, the target could be expressed either as a vector, containing the spatial coordinates of the target location or as an image, showing the object in the desired pose and location.

After analyzing the causes of failure in this setup, we

propose two solutions to improve performance: a simpler solution that applies to any world model architecture and a more tailored solution for object-centric world models. Finally, we evaluate the proposed methods over a set of object positioning tasks, showing a neat improvement over standard methods. To summarize, the contributions of this work are as follows:

- an analysis of the reasons for the inefficiency of generative model-based agents for solving tasks that require positional information;
- a simpler solution that presents no major changes to the world model architecture and minimal changes to policy learning. This solution already strongly improves performance in several tasks, where the target is expressed as a vector of spatial coordinates;
- a tailored solution employing an object-centric approach that integrates positional information about the objects into the latent space of the world model. This approach enables the possibility to specify goals through multimodal targets, e.g. vector inputs or visual goals.

## Preliminaries

The agent is a robotic manipulator that, at each discrete timestep  $t$  receives an input  $x_t$  from the environment. The goal of the agent is to move an object in the environment from its current position  $p_t^{obj}$  to a target goal position  $p_g^{obj}$ .

In this work, we focus on observations composed of both visual and vector entities. Thus,  $x_t = (o_t, v_t)$  is composed of the visual component  $o_t$  and of the vector  $v_t$ . The latter is a concatenation of proprioceptive information of the robotic manipulator  $q_t$ , the object’s position  $p_t^{obj}$ , and the target position  $p_g^{obj}$ . The target position can also be expressed through a visual observation  $x_g$ , from which the agent should infer the corresponding  $p_g^{obj}$  to succeed in the positioning task.

## Generative World Models

Generative world models learn a latent representation of the agent inputs using a variational auto-encoding framework (Kingma and Welling 2022). Dreamer-like agents (Hafner et al. 2021, 2023) implement the world model as a Recurrent State-Space Model (RSSM) (Hafner et al. 2019). The encoder  $f(\cdot)$  is instantiated as the concatenation of the outputs of a CNN for high-dimensional observations and an MLP for low-dimensional proprioception. Through the encoder network, the input  $x_t$  is mapped to an embedding  $e_t$ , which then is integrated with dynamical information with respect to the previous RSSM state and the action taken  $a_t$ , resulting in  $s_t$  features.

$$\begin{aligned} \text{Encoder: } e_t &= f(x_t) \\ \text{Posterior: } p_\phi(s_{t+1}|s_t, a_t, e_{t+1}), \\ \text{Prior: } p_\phi(s_{t+1}|s_t, a_t), \\ \text{Decoder: } p_\theta(\hat{x}_t|s_t). \end{aligned}$$

Generally, the system either learns to predict the expected reward given the latent features (Hafner et al. 2020), using a reward predictor  $p_\theta(\hat{r}_t|s_t)$ . Alternatively, some world-model

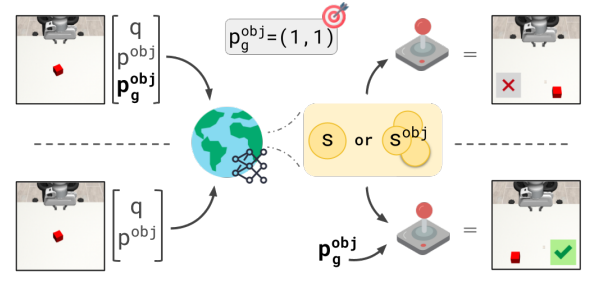


Figure 2: The **world model** compresses visual observations and state vector into a latent state representation. Crucially, the compressed representation serves as input to the policy for action selection. The world model can either be **flat**, encoding a single latent state, or **object-centric**, where the latent representation consists of distinct latent states for each object. **(top)** Goal information is provided through the input state vector. **(bottom)**: Both single and object-centric representations can be paired to a **target-conditioned policy**.

based methods adopt specialized ways to compute rewards in imagination, as the goal-conditioned objectives in LEXA (Mendonca et al. 2021).

Rewards are computed on rollouts of latent states generated by the model and are used to learn the policy  $\pi$  and value network  $v$  in imagination (Hafner et al. 2020, 2021, 2023).

In our experiments, we consider a world model with a discrete latent space (Hafner et al. 2021). We also implement advancements of the world model representation introduced in DreamerV3 (Hafner et al. 2023), such as the application of the symlog transform to the inputs, KL balancing, and free bits to improve the predictions of the vector inputs and the robustness of the model.

## Object-centric World Models

Compared to Dreamer-like *flat* world models, the world model of FOCUS (Ferraro et al. 2023) introduces the following object-centric components:

$$\begin{aligned} \text{Object latent extractor: } p_\theta(s_t^{obj}|s_t, c^{obj}), \\ \text{Object decoder: } p_\theta(\hat{x}_t^{obj}, \hat{m}_t^{obj}|s_t^{obj}). \end{aligned}$$

Here,  $x_t^{obj} = (o_t^{obj}, p_t^{obj})$  represents the object-centric inputs and it is composed of segmented RGB images  $o_t^{obj}$  and object positions  $p_t^{obj}$ . The variable  $c^{obj}$  indicates which object is being considered.

Thanks to the *object latent extractor* unit, object-specific information is separated into distinct latent representations  $s_t^{obj}$ . Two decoding units are present. The introduced object-centric decoder  $p_\theta(\hat{x}_t^{obj}, \hat{m}_t^{obj}|s_t^{obj})$  reconstructs each object’s related inputs  $x_t^{obj}$  and segmentation mask  $m_t^{obj}$ . The original Dreamer-like decoder takes care of the reconstruction of the remaining vector inputs, i.e. proprioception  $q_t$  and given goal targets  $p_g^{obj}$ .

We provide additional descriptions of the world model and policy learning losses, hyperparameters, and training details in the Appendix.

## Object Positioning Tasks

In general terms, we consider positioning tasks the ones where an entity of interest has to be moved to a specific location. Two positioning scenarios are considered in this analysis: *pose reaching* and *object positioning*. Pose-reaching tasks can be seen as simplified positioning tasks where the entity of interest is part of the robotic manipulator itself. Pose-reaching tasks are interesting because these only require the agent to have knowledge of the proprioceptive information to infer their position in space and reach a given target. When interacting with objects instead, there is the additional necessity of knowing the position of the object entity in the environment. Then, the agent needs to be able to manipulate and move the entity to the provided target location.

For object positioning tasks, especially when considering a real-world setup, there is a significant advantage in relying mainly on visual inputs. It is convenient because it avoids the cost and difficulty associated with tracking additional state features, such as the geometrical shape of objects in the scene or the presence of obstacles. Some synthetic benchmarks additionally make use of "virtual" visual targets for positioning tasks (Tunyasuvunakool et al. 2020; Yu et al. 2019), which strongly facilitates the learning of these tasks, leveraging rendering in simulation. However, applying such "virtual" targets in real-world settings is not often feasible. Non-visual target locations can be provided as spatial coordinates. Alternatively, an image showing the target location could be used to specify the target's position.

**Rewards and evaluation criteria.** When applying RL algorithms to a problem, a heavily engineered reward function is generally necessary to guide the agent's learning toward the solution of the task (OpenAI et al. 2019). The object positioning setup allows us to consider a natural and intuitive reward definition that scales across different agents and environments. We define the reward as the negative distance between the position of the entity of interest and the goal target position:

$$r_t = -\text{distance}(\text{object}, \text{target}) = -\|p_t^{\text{obj}} - p_g^{\text{obj}}\|_2. \quad (1)$$

In the spirit of maintaining a setup that is as close as possible to a real-world one, to retrieve positional information  $p_t$  of the objects we rely on image segmentation information, rather than using the readings provided from the simulator. For each entity of interest, the related position is extracted by computing the centroid of the segmentation mask and subsequently transformed according to the camera extrinsic and intrinsic matrices to obtain the absolute position with respect to the workspace.

For evaluation purposes, we use the goal-normalized score function:

$$\text{normalized score} = \exp\left(-\frac{\|p_t^{\text{obj}} - p_g^{\text{obj}}\|_2}{\|p_g^{\text{obj}}\|_2}\right) \quad (2)$$

As detailed in the Appendix, the above function allows us to rescale performance between 0 and 1, where 1 = expert performance, a common evaluation strategy in RL (Cobbe et al. 2020; Fan 2023).

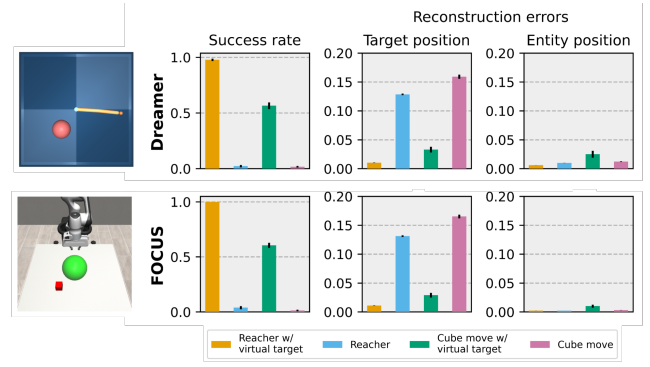


Figure 3: **left:** examples of virtual targets visualization. **top-right:** Dreamer’s success rate and reconstruction performance over target and entity position (end-effector performance for the cube move environment). **bottom-right:** Equivalent for the FOCUS object-centric model. The success rate for both environments is defined as the entity of interest being within 5cm from the given target at the termination of the episode. Reconstruction errors are computed as L2-norm.

## Analysis of the Current Limitations

To provide insights into the limitations of current world model-based agents in object-positioning tasks, we consider the performance of Dreamer and FOCUS on a pose-reaching and an object-positioning task.

For pose-reaching, we opted for the Reacher environment from the DMC suite (Tunyasuvunakool et al. 2020). In this task, we consider the end-effector of the manipulator as the entity to be positioned at the target location. For the more complex object positioning task, we opted for a cube-manipulation task from Robosuite (Zhu et al. 2020). The given cube has to be placed at the specified target location to succeed in the task.

In both environments, the target position is uniformly sampled within the workspace at every new episode. We test the environments in two different scenarios: first, with a virtual visual target that is rendered in the environment, and second, without a visual target, where the target location is provided only as a vector in the agent’s inputs.

Dreamer and FOCUS agents are trained for 250k gradient steps on both environments in an offline RL fashion. Datasets of 1M steps are collected adopting the exploration strategy presented in (Ferraro et al. 2023). Both the world model and the policy are updated at every training step. In Figure 3, we present an overview of the agents’ success rate and of the capabilities at reconstructing positional information.

We make the following observations:

- The agents’ performance is comparable, with FOCUS being slightly more successful and more accurate in predicting the target and entity position. This is likely thanks to the object-centric nature of the approach;
- There is a significant gap in performance between the tasks with the virtual visual targets rendered in the environment and the tasks using only spatial coordinates as

a target. The agents struggle to solve the tasks without a virtual target;

- There is a negative correlation between the agents’ ability to reconstruct positional information and the performance on the task. The lower the reconstruction errors, the higher the success rate on the task. This is particularly evident for the target position, but it also seems to apply to the entity position, i.e. might be the reason for FOCUS performing better than Dreamer.

In the remainder of this section, we aim to provide an explanation for the above observations.

**Why is the visual cue so important?** There is a significant difference in the relative significance of the target information compared to the entire observation, in terms of their dimensionality. The information pertaining to a positional target comprises a maximum of three values (i.e., the  $xyz$  coordinates of the target). Conversely, when considering a visual cue, there are three values (i.e., RGB values) for each pixel that represents the target cue. Consequently, the relative significance of the target information is, at least, greater in the case of a large visual target, i.e. larger than a single pixel. This difference in the dimensionality affects the computation of the loss, and thus the weight of each component in the decoder’s loss. For the entity, the agents have access to this information in the visual observation. Indeed, it’s not surprising that both agents reconstruct the entity position accurately.

**Size matters!** To confirm our hypothesis that the improved predictions are due to the greater significance of the visual targets in the overall loss, we provide additional experiments. In Figure 4, we present a study where the Dreamer model is trained on the Reacher environment with varying visual target sizes. We observe that the reduction in pixel information regarding the target adversely affects the target representation within the model, resulting in a deficiency of this information being conveyed to the policy network. The policy struggles to learn to position the entity at the correct location, and we observe that this is correctly reflected in the value function’s predictions. This means the policy is aware that is not being able to reach the goal. With small targets ( $< 5$  pixels diameters), the representation tends to put more attention on other visually predominant aspects of the environment, struggling to predict the position of the target. In the case of a single pixel target, the amount of target information equals the one

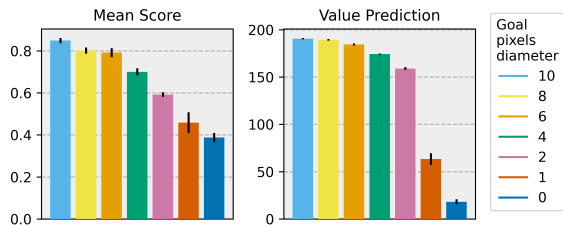


Figure 4: Dreamer virtual visual goal modulation experiments on the Reacher environment. Value prediction from the value network is shown to highlight the policy’s awareness of the lack of information with respect to the target goal.

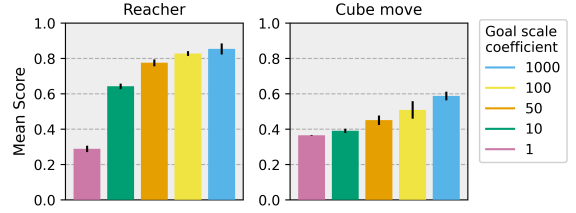


Figure 5: Dreamer trained with goal scaling modulation on the Reacher and Cube move environments.

of a positional vector and, as expected, the task performance is equally low.

**Loss rescaling.** To overcome the identified information bottleneck, different strategies can be considered. The simplest one is the re-scaling of the loss components in the decoder to incentivize the model’s encoding of the target information. This approach requires finding the optimal scaling factor between the different decoding components, given the complexity of the environment at hand (i.e. 2D or 3D) and the amount of relevant pixels. In Figure 5, we present supporting experiments based on Dreamer, where we vary the importance of the target in the loss of the world model, using different coefficients. We observe that very high coefficients improve the target’s reconstruction and thus allow the agent to learn the task. However, the optimal loss coefficient may vary, depending on the complexity of the environment and the presence of information-rich observations. As this naive solution may require extensive hyperparameter tuning for each new scenario, we aim to find more robust strategies for overcoming this issue.

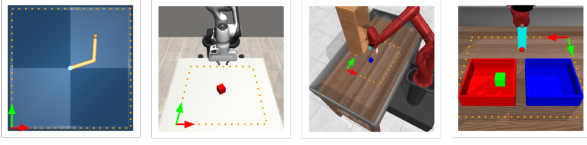
**Discussion.** Adjusting loss coefficients is a common practice in machine learning. A concurrent work (Ma et al. 2024) conducted an extensive study between the interplay of the reward and the observation loss in a world model. Our analysis provides an additional insight, as we identify within the observation loss, an unbalance between the different decoded components. In this work, rather than focussing on how to balance the losses, we consider different approaches to alleviate this issue. The central idea is to find alternative ways to provide positional information about the target directly to the reward computation and policy learning modules, rather than relying on the reconstruction of the targets obtained by the model.

## Position Conditioned Policy (PCP)

The first declination of our proposed solutions is the conditioning of the policy directly on the positional coordinates of the desired target. By default, the world model encodes the target’s positional information in the latent states, which are then fed to the policy for behavior learning. Instead, as shown in the bottom of Figure 2, we propose to concatenate the object positional coordinates  $p_g^{obj}$  to the latent states  $s_t$  as an input to the policy network  $\pi_{PCP}$ .







	Dreamer	FOCUS	Dreamer + PCP	FOCUS + PCP	FOCUS + LCP
Reacher	$0.27 \pm 0.11$	$0.29 \pm 0.1$	$0.8 \pm 0.08$	$0.87 \pm 0.04$	<b><math>0.91 \pm 0.02</math></b>
Cube move	$0.35 \pm 0.05$	$0.35 \pm 0.08$	$0.54 \pm 0.04$	<b><math>0.75 \pm 0.04</math></b>	<b><math>0.73 \pm 0.05</math></b>
Shelf place	$0.4 \pm 0.06$	$0.3 \pm 0.1$	$0.58 \pm 0.08$	$0.59 \pm 0.1$	<b><math>0.70 \pm 0.08</math></b>
Pick&Place	$0.26 \pm 0.13$	$0.22 \pm 0.12$	<b><math>0.48 \pm 0.15</math></b>	<b><math>0.48 \pm 0.17</math></b>	<b><math>0.43 \pm 0.18</math></b>
Overall	$0.32 \pm 0.08$	$0.29 \pm 0.09$	$0.6 \pm 0.09$	<b><math>0.67 \pm 0.09</math></b>	<b><math>0.7 \pm 0.08</math></b>

Table 1: Average score for 100 goal points equally distributed over the workspace. For each task, the environments are shown, in order, on the left. We also show the goal points’ workspace, delimited by an orange dotted line, and the reference frames indicated with arrows. Performance is averaged over 3 seeds,  $\pm$  indicates the standard error.

## Baselines and Environments

For the evaluation of the proposed method we consider several manipulation environments:

- **Reacher** (DMControl): which, as described previously, represents a pose-reaching positioning task.
- **Cube move** (Robosuite): where considered target locations are on the 2D plane of the table, no height placement is considered.
- **Shelf place** and **Pick&Place** (Metaworld): The robotic manipulator has to place the cube at the given target location. Considered target locations are on the 2D space in front of the robotic arm.

In all environments, the reward signal is defined as the distance between the entity of interest (in the Reacher environment, this is the end-effector) and the target location. All considered environments lack any visual target; the target is provided as an input vector containing spatial coordinates.

We benchmark our methods against various baselines:

- **Dreamer**: based on a PyTorch DreamerV2 implementation, but integrated with input vector symlog transformation and KL balancing of the latent dynamic representation, from the DreamerV3 paper.
- **FOCUS**: An object-centric world model implementation based on DreamerV2, also integrated with input vector symlog transformation and KL balancing of the latent dynamic representation.
- **LEXA**: Based on DreamerV2, this is a latent goal-conditioned method. The conditioning is based on the full latent target. Both proposed distance methods (cosine and temporal) are considered. We adopted our own PyTorch implementation for LEXA.

All methods are trained following an offline RL training scheme. The offline datasets contain 1M steps in the environment, which are collected using the object-centric exploration strategy proposed in (Ferraro et al. 2023). Each model is trained on the dataset for 250K steps, with both the world model and policy network updated at each training step.

## Results

We now present the evaluation of the trained models. The main metric considered is the score function presented in Equation 5. With the experiments, we want to verify whether the introduced techniques, PCP and LCP, overcome the issues presented with object positioning tasks for generating world model-based agents.

First, we verify the performance achieved by the methods when adopting spatial coordinates for the goal definition. We benchmark Dreamer with PCP and FOCUS both with PCP and LCP, and we compare them with the standard Dreamer and FOCUS agents.

Then, we study the FOCUS + LCP method more in detail, by analyzing its multimodal goal specification capabilities. We show a set of experiments where the goal is provided in a visual fashion, using observations with the object positioned at the target location. Here, we compare FOCUS + LCP against the two implementations of LEXA, cosine and temporal.

### Spatial-coordinates goal specification

By providing the different agents with goals uniformly distributed in the workspace we extract the overall performance of each method. Results are presented in Table 1.

Overall, the FOCUS agent equipped with PCP or LCP gives the best performance, followed by Dreamer + PCP. In the “Shelf place” environment, the latent representation of LCP represents best. Given that the camera is further away

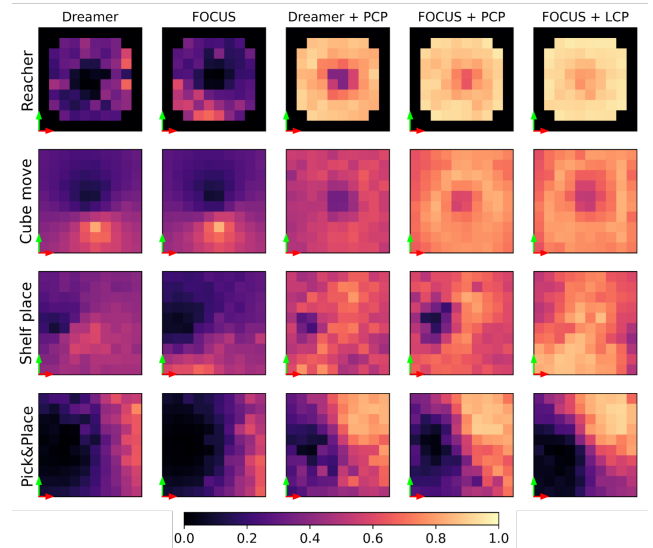


Figure 7: Heatmaps of the mean achieved score for uniformly spread targets in the workspace. References frames refers to the one presented in the figures of Table 1. The score notation is expressed as the notation presented in Eq. 2. Results are averaged over 3 seeds.

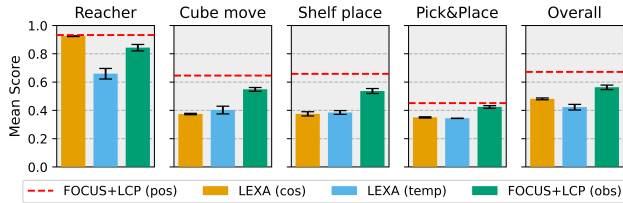


Figure 8: **Visual goals.** The mean score was achieved over 10 episodes with goal observations for latent conditioning. LEXA is tested both for the cosine and temporal variation. The performance of our method with spatial-coordinate goals (pos) is shown as a reference. The score is expressed according to Equation 2.

from the scene, we believe the agent is better able to deal with the inaccuracies that come from the inaccurate position readings (bigger segmentation mask  $\rightarrow$  better granularity in position).

We also observe that the FOCUS + PCP position is superior to Dreamer + PCP. This is a similar observation as in our analysis of the limitations, where FOCUS tended to perform better than Dreamer. The more accurate predictions of the entity position, in object-centric world models, might be the source of the improved performance.

Finally, as expected, the performance of Dreamer and FOCUS is insufficient in all tasks, and much lower than their PCP and LCP counterparts.

To highlight the performance distribution over the different goals in the environment, in Fig. 7 we present heatmaps with the score function for each target location in the workspace. Results are presented for all the different tasks. As expected, both Dreamer and FOCUS have poor performances, resulting in only a few positions being reached with a high score. All the proposed methods have a similar distribution, reaching goals spread all over the environment.

## Visual goal specification

An interesting emergence property of FOCUS + LCP is the possibility to define goals via different modalities. The policy  $\pi_{LCP}$  can be conditioned on the goal object latent  $\hat{s}_g^{obj}$  coming from the encoding of the visual goal  $x_g$ . LEXA (Mendonca et al. 2021) also adopts visual goals for conditioning the action policy, but allows no fine-grained specification of the goal. Thus, to match the goal the agent should accomplish both the agent’s pose and the objects’ positions from the visual goal. This makes the task harder to accomplish than for our method, where the agent can simply focus on the objects’ positions. LEXA temporal is designed to overcome this issue, but it generally requires more data to converge (Mendonca et al. 2021).

We compare our method with visual goal conditioning against LEXA cosine and temporal. The goal locations are provided to the simulator which renders the corresponding goal observations by “teleporting” the object to the correct location. The agent is then asked to match the visual goal, after resetting the environment. Results are shown in Fig.

8, where the positional conditioning results are shown for reference.

As stated before, LEXA matches the flat latent vector to the goal one. This proves helpful in the Reacher environment, where the only part that moves is the agent, and thus LEXA cosine achieves the best performance. LEXA cosine fails in the other tasks, given the presence of multiple entities in the observations and visual goals, i.e. the robotic arm and the object, where the model focuses on matching the visually predominant features i.e. the robotic arm.

LEXA temporal is found to generally underperform. We hypothesize this is due to the need for a larger training dataset, as the training signal, the temporal distance, is less informative than the latent distance, and thus requires more samples from the environment.

FOCUS+LCP performs better than both LEXA with cosine and temporal distance in all environments but the Reacher. When compared to the performance of FOCUS+LCP with spatial-coordinates goal specification, there is a decrease of only  $\sim 10\%$  in performance. This shows that the approach is promising as a multimodal goal specification method.

## Conclusion

We analyzed the challenges in solving visual robotic positional tasks using generative world model-based agents. We found these systems suffer from information bottleneck issues when considering positional information for task resolution. Under-represented information is challenging for the model to encode, especially in the case of not stationary values such as a variable target.

The approaches we presented overcome this issue by providing the policy network with more direct access to the target information. Two declinations are proposed. The first, the Positional Conditioning Policy (PCP), allows direct conditioning on the target spatial coordinates. We showed PCP improves performance for any class of world models, including Dreamer-like “flat” world models and FOCUS-like object-centric world models. The second declination, Latent Conditioning Policy (LCP), is an object-centric approach that we implement on top of FOCUS. This allows the conditioning of the policy on object-centric latent targets.

As future work, it would be interesting to analyze the application of such approaches to non-positional features, such as a shape (e.g. object deformation) or object configuration (e.g. open/close faucet, light on/off). Moreover, it would be interesting to scale the application of LCP to other modalities. For instance, one could consider multimodal inputs including both visual and tactile observations.

## References

- Andrychowicz, M.; Wolski, F.; Ray, A.; Schneider, J.; Fong, R.; Welinder, P.; McGrew, B.; Tobin, J.; Abbeel, P.; and Zaremba, W. 2018. Hindsight Experience Replay. arXiv:1707.01495.
- Cobbe, K.; Hesse, C.; Hilton, J.; and Schulman, J. 2020. Leveraging Procedural Generation to Benchmark Reinforcement Learning. arXiv:1912.01588.

- Fan, J. 2023. A Review for Deep Reinforcement Learning in Atari: Benchmarks, Challenges, and Solutions. *arXiv:2112.04145*.
- Ferraro, S.; Mazzaglia, P.; Verbelen, T.; and Dhoedt, B. 2023. FOCUS: Object-Centric World Models for Robotics Manipulation. *arXiv:2307.02427*.
- Fujimoto, S.; van Hoof, H.; and Meger, D. 2018. Addressing Function Approximation Error in Actor-Critic Methods. *arXiv:1802.09477*.
- Ha, D.; and Schmidhuber, J. 2018. World Models.
- Haarnoja, T.; Zhou, A.; Abbeel, P.; and Levine, S. 2018. Soft Actor-Critic: Off-Policy Maximum Entropy Deep Reinforcement Learning with a Stochastic Actor. *arXiv:1801.01290*.
- Hafner, D.; Lillicrap, T.; Ba, J.; and Norouzi, M. 2020. Dream to Control: Learning Behaviors by Latent Imagination.
- Hafner, D.; Lillicrap, T.; Fischer, I.; Villegas, R.; Ha, D.; Lee, H.; and Davidson, J. 2019. Learning Latent Dynamics for Planning from Pixels. In *ICML*, 2555–2565.
- Hafner, D.; Lillicrap, T. P.; Norouzi, M.; and Ba, J. 2021. Mastering Atari with Discrete World Models. In *ICLR*.
- Hafner, D.; Pasukonis, J.; Ba, J.; and Lillicrap, T. 2023. Mastering Diverse Domains through World Models. *arXiv preprint arXiv:2301.04104*.
- Hansen, N.; Su, H.; and Wang, X. 2024. TD-MPC2: Scalable, Robust World Models for Continuous Control.
- Hansen, N.; Wang, X.; and Su, H. 2022. Temporal Difference Learning for Model Predictive Control. *arXiv:2203.04955*.
- Kalashnikov, D.; Irpan, A.; Pastor, P.; Ibarz, J.; Herzog, A.; Jang, E.; Quillen, D.; Holly, E.; Kalakrishnan, M.; Vanhoucke, V.; and Levine, S. 2018. QT-Opt: Scalable Deep Reinforcement Learning for Vision-Based Robotic Manipulation. *ArXiv*, abs/1806.10293.
- Kingma, D. P.; and Welling, M. 2022. Auto-Encoding Variational Bayes. *arXiv:1312.6114*.
- Lancaster, P.; Hansen, N.; Rajeswaran, A.; and Kumar, V. 2024. MoDem-V2: Visuo-Motor World Models for Real-World Robot Manipulation. *arXiv:2309.14236*.
- Lee, A. X.; Devin, C.; Zhou, Y.; Lampe, T.; Bousmalis, K.; Springenberg, J. T.; Byravan, A.; Abdolmaleki, A.; Gileadi, N.; Khosid, D.; Fantacci, C.; Chen, J. E.; Raju, A. S.; Jeong, R.; Neunert, M.; Laurens, A.; Saliceti, S.; Casarini, F.; Riedmiller, M. A.; Hadsell, R.; and Nori, F. 2021. Beyond Pick-and-Place: Tackling Robotic Stacking of Diverse Shapes. *ArXiv*, abs/2110.06192.
- Levine, S.; Finn, C.; Darrell, T.; and Abbeel, P. 2016. End-to-End Training of Deep Visuomotor Policies. *J. Mach. Learn. Res.*
- Lu, Y.; Hausman, K.; Chebotar, Y.; Yan, M.; Jang, E.; Herzog, A.; Xiao, T.; Irpan, A.; Khansari, M.; Kalashnikov, D.; and Levine, S. 2021. AW-Opt: Learning Robotic Skills with Imitation and Reinforcement at Scale. In *5th Annual Conference on Robot Learning (CoRL)*.
- Ma, H.; Wu, J.; Feng, N.; Xiao, C.; Li, D.; Hao, J.; Wang, J.; and Long, M. 2024. HarmonyDream: Task Harmonization Inside World Models. *arXiv:2310.00344*.
- Mendonca, R.; Rybkin, O.; Daniilidis, K.; Hafner, D.; and Pathak, D. 2021. Discovering and Achieving Goals via World Models. *arXiv:2110.09514*.
- OpenAI; Akkaya, I.; Andrychowicz, M.; Chociej, M.; Litwin, M.; McGrew, B.; Petron, A.; Paino, A.; Plappert, M.; Powell, G.; Ribas, R.; Schneider, J.; Tezak, N. A.; Tworek, J.; Welinder, P.; Weng, L.; Yuan, Q.; Zaremba, W.; and Zhang, L. M. 2019. Solving Rubik’s Cube with a Robot Hand. *ArXiv*, abs/1910.07113.
- Rajeswar, S.; Mazzaglia, P.; Verbelen, T.; Piché, A.; Dhoedt, B.; Courville, A.; and Lacoste, A. 2023. Mastering the Unsupervised Reinforcement Learning Benchmark from Pixels.
- Schaul, T.; Horgan, D.; Gregor, K.; and Silver, D. 2015. Universal value function approximators. In *International conference on machine learning*, 1312–1320. PMLR.
- Sekar, R.; Rybkin, O.; Daniilidis, K.; Abbeel, P.; Hafner, D.; and Pathak, D. 2020. Planning to Explore via Self-Supervised World Models. In *ICML*.
- Seo, Y.; Hafner, D.; Liu, H.; Liu, F.; James, S.; Lee, K.; and Abbeel, P. 2022. Masked World Models for Visual Control. *arXiv:2206.14244*.
- Seo, Y.; Kim, J.; James, S.; Lee, K.; Shin, J.; and Abbeel, P. 2023. Multi-View Masked World Models for Visual Robotic Manipulation. *arXiv:2302.02408*.
- Tunyasuvunakool, S.; Muldal, A.; Doron, Y.; Liu, S.; Bohez, S.; Merel, J.; Erez, T.; Lillicrap, T.; Heess, N.; and Tassa, Y. 2020. dm.control: Software and tasks for continuous control. *Software Impacts*, 6: 100022.
- Wu, P.; Escontrela, A.; Hafner, D.; Goldberg, K.; and Abbeel, P. 2022. DayDreamer: World Models for Physical Robot Learning. *arXiv:2206.14176*.
- Yu, T.; Quillen, D.; He, Z.; Julian, R.; Hausman, K.; Finn, C.; and Levine, S. 2019. Meta-World: A Benchmark and Evaluation for Multi-Task and Meta Reinforcement Learning. In *Conference on Robot Learning (CoRL)*.
- Zhu, Y.; Wong, J.; Mandlekar, A.; Martín-Martín, R.; Joshi, A.; Nasiriany, S.; and Zhu, Y. 2020. robosuite: A Modular Simulation Framework and Benchmark for Robot Learning. In *arXiv preprint arXiv:2009.12293*.



## Supplementary Material

### Normalized score

Scaling performance using expert performance is a common evaluation strategy in RL (Cobbe et al. 2020; Fan 2023). In our problem, we define the reward as the negative distance:

$$r_t = -r(p_t^{obj}) = -\|p_t^{obj} - p_g^{obj}\|_2. \quad (5)$$

For a given goal  $p_g^{obj}$ ,  $r_t \in ] - \inf, 0]$ . In order to compare different tasks, where distances may have different magnitudes, we divide the rewards  $r_t$  by the typical reward range. This is given by  $r_{max} - r_{min}$ , where  $r_{min} = r(p_0^{obj})$ , with  $p_0$  being the initial position of the object (this is normally around the origin, and  $r_{max} = r(p_g^{obj}) = 0$ ).

Thus, we obtain:

$$s_t = r_t / (r_{max} - r_{min}) \quad (6)$$

$$= r(p_t^{obj}) / (0 - r(p_0^{obj})) = \quad (7)$$

$$= -\|p_t^{obj} - p_g^{obj}\|_2 / (0 + \|p_0 - p_g^{obj}\|_2) \quad (8)$$

$$= -\|p_t^{obj} - p_g^{obj}\|_2 / \|p_g^{obj}\|_2 \quad (9)$$

Finally, we apply the exp operator, to make values positive and bring them in the  $[0, 1]$  range, where 1 is the expert score:

$$\text{normalized score} = \exp\left(-\frac{\|p_t^{obj} - p_g^{obj}\|_2}{\|p_g^{obj}\|_2}\right) \quad (10)$$

### FOCUS objective

Training of the FOCUS architecture is guided by the following loss function:

$$\mathcal{L}_{\text{FOCUS}} = \mathcal{L}_{\text{dyn}} + \mathcal{L}_{\text{state}} + \mathcal{L}_{\text{obj}}. \quad (11)$$

$\mathcal{L}_{\text{dyn}}$  refers to the dynamic component of the RSSM, and equals too:

$$\mathcal{L}_{\text{dyn}} = D_{\text{KL}}[p_\phi(s_{t+1}|s_t, a_t, e_{t+1}) || p_\phi(s_{t+1}|s_t, a_t)]. \quad (12)$$

the backpropagation is balanced and clipped below 1 nat as in DreamerV3 (Hafner et al. 2023).

The object loss component is instantiated as the composition of NLL over the mask and RGB mask reconstructions:

$$\mathcal{L}_{\text{obj}} = -\log \underbrace{p(\hat{m}_t)}_{\text{mask}} - \log \sum_{\text{obj}=0}^N \underbrace{m_t^{\text{obj}} p_\theta(\hat{x}_t^{\text{obj}} | s_t^{\text{obj}})}_{\text{masked reconstruction}} \quad (13)$$

Finally, the decoder learns to reconstruct the rest of vector state information  $v_t$  by minimization of the negative log-likelihood (NLL) loss:

$$\mathcal{L}_{\text{state}} = -\log p_\theta(\hat{q}_t, p_g^{obj} | s_t) \quad (14)$$

### Training details and Hyperparameters

All models in the presented work have been trained offline. Datasets have been collected beforehand, guided by the exploration agent of choice (we tested both the Object-centric entropy maximization proposed in FOCUS (Ferraro et al.

2023) and Plan2Explore (Sekar et al. 2020)). The datasets are loaded in the replay buffer of the offline agents, and the training is conducted for 250K steps. Both world model and agent are updated at every training step. V100-16GB GPUs have been used for all experiments. Our proposed methods (i.e. Dreamer/FOCUS + PCP, FOCUS + LCP) took roughly 18 hours to complete each training run.

The hyperparameters used for the main implementation of the world models and agent are the same used in DreamerV2 (Hafner et al. 2021) official implementation. Symlog function is applied at every input. KL balancing as in DreamerV3 (Hafner et al. 2023) is implemented.

With reference to FOCUS model, we have the following additional parameters:

- Object-extractor: MLP composed of 2 layers, 512 units, ReLU activation;

With reference to FOCUS + LCP model, we have the following additional parameters:

- Object-encoder: MLP composed of 4 layers, 400 units, ReLU activation;
- Distance method object-encoder objective: Cosine similarity (also tested MSE)
- Distance method actor policy objective: Cosine similarity (also tested MSE)

### Offline Training Curves

Offline training curves are presented in Figure 9. In general FOCUS + PCP/LCP have faster convergence when compared to all other methods. Only for the Reacher environment, LEXA cosine converge faster.

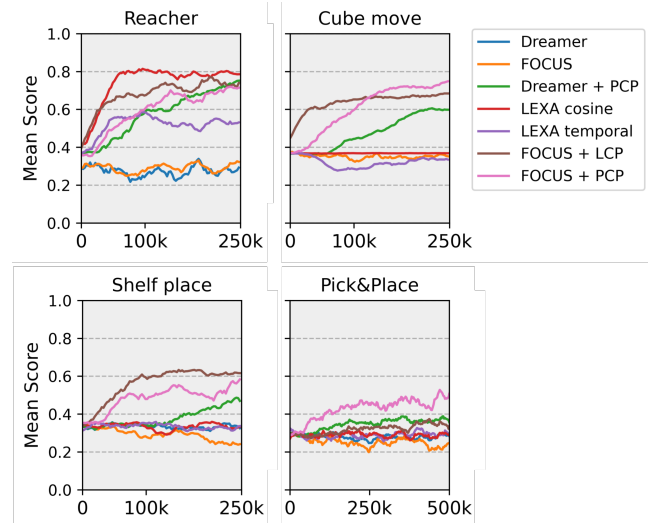


Figure 9: Offline training curves. Standard deviation is omitted for graphical reasons. Mean score refers to eq. 2

and is computed over 5 evaluation episodes, performed during the offline training. For each episode, a random goal is selected out of a pool of 10 manually engineered ones.

## Explorations strategies

In the presented work each model is trained offline from a pre-recorded dataset. The dataset of choice is obtained from pure exploration behavior. In Fig. 10 we compare the general performance of LCP when trained on datasets acquired using different exploration strategies. We consider the object-centric entropy maximization method proposed by Ferraro et al. (Ferraro et al. 2023) and Plan2Explore (Sekar et al. 2020).

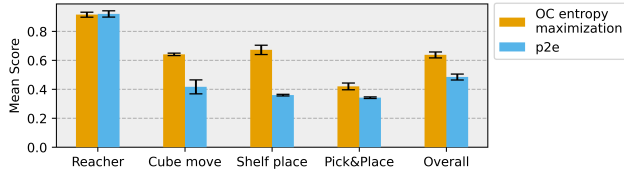


Figure 10: Mean score achieved over 10 episodes for models trained with both datasets obtained from FOCUS exploration method (Object-Centric entropy maximization) and Plan2Explore. The score is expressed according to equation 2.

Overall exploring by maximizing the entropy over the object’s latent, gives better performance in the downstream task. We hypothesize this is related to the focus the exploration strategy puts on the object of interest while disregarding background aspects in the scene.

## Reproducibility Checklist

This paper:

- Includes a conceptual outline and/or pseudocode description of AI methods introduced (yes)
- Clearly delineates statements that are opinions, hypothesis, and speculation from objective facts and results (yes)
- Provides well marked pedagogical references for less-familiar readers to gain background necessary to replicate the paper (yes)

Does this paper make theoretical contributions? (no)

Does this paper rely on one or more datasets? (no)

Does this paper include computational experiments? (yes)

If yes, please complete the list below.

- Any code required for pre-processing data is included in the appendix. (yes).
- All source code required for conducting and analyzing the experiments is included in a code appendix. (yes)
- All source code required for conducting and analyzing the experiments will be made publicly available upon publication of the paper with a license that allows free usage for research purposes. (yes)
- All source code implementing new methods have comments detailing the implementation, with references to the paper where each step comes from (partial)
- If an algorithm depends on randomness, then the method used for setting seeds is described in a way sufficient to allow replication of results. (yes)
- This paper specifies the computing infrastructure used for running experiments (hardware and software), including GPU/CPU models; amount of memory; operating system; names and versions of relevant software libraries and frameworks. (yes)
- This paper formally describes evaluation metrics used and explains the motivation for choosing these metrics. (yes)
- This paper states the number of algorithm runs used to compute each reported result. (yes)
- Analysis of experiments goes beyond single-dimensional summaries of performance (e.g., average; median) to include measures of variation, confidence, or other distributional information. (yes)
- The significance of any improvement or decrease in performance is judged using appropriate statistical tests (e.g., Wilcoxon signed-rank). (partial)
- This paper lists all final (hyper-)parameters used for each model/algorithm in the paper's experiments. (yes)
- This paper states the number and range of values tried per (hyper-) parameter during development of the paper, along with the criterion used for selecting the final parameter setting. (NA)